

Joint Pathology Center
Veterinary Pathology Services

WEDNESDAY SLIDE CONFERENCE
2020-2021

Conference 7

7 October 2020



Joint Pathology Center
Silver Spring, Maryland

CASE 1: A19-490A (4153162-00)

Signalment:

Adult, male, brown anole (*Anolis sagrei*)

History:

Multiple, free ranging brown anoles in western, central Florida, United States were observed to have multiple raised, disfiguring subcutaneous masses and facial swellings. Over the course of several months, six affected individuals were collected and submitted for post-mortem examination. The submitted photographs, photomicrographs, and histologic sections are from one of these animals. The findings were similar across all six individuals.

Gross Pathology:

Along the head, trunk, dorsal pelvic region, hindlimbs, and tail, there are tens of multifocal to coalescing, subcutaneous, fluctuant masses, which range from approximately 2 x 2 x 2 mm to 6 x 6 x 4 mm. A few of the masses are superficially ulcerated and one on the ventrolateral aspect of the thoracic body wall is deeply ulcerated. On cut section, the masses are white, opaque, and gelatinous. There is also an ill-defined swelling surrounding the caudoventral aspect of the left mandible, which extends to the left tympanum. The gross internal examination is unremarkable.

The submitted slides include sections from the masses on the tail and one of the hindlimbs.

Laboratory results:

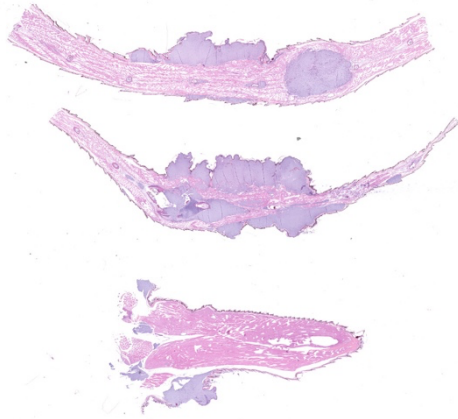
PCR (16S and 16S-23S IGS): 100% sequence identity to a novel *Enterococcus* sp. reported in reptiles from Christmas Island

Microscopic description:

Multifocally elevating the epidermis and infiltrating and expanding the dermis, subcutis, skeletal muscle, and vertebral bone, there are several large, mass-like aggregates of numerous coccoid bacteria. The bacteria are less than 1 micrometer in diameter, and they form distinct,



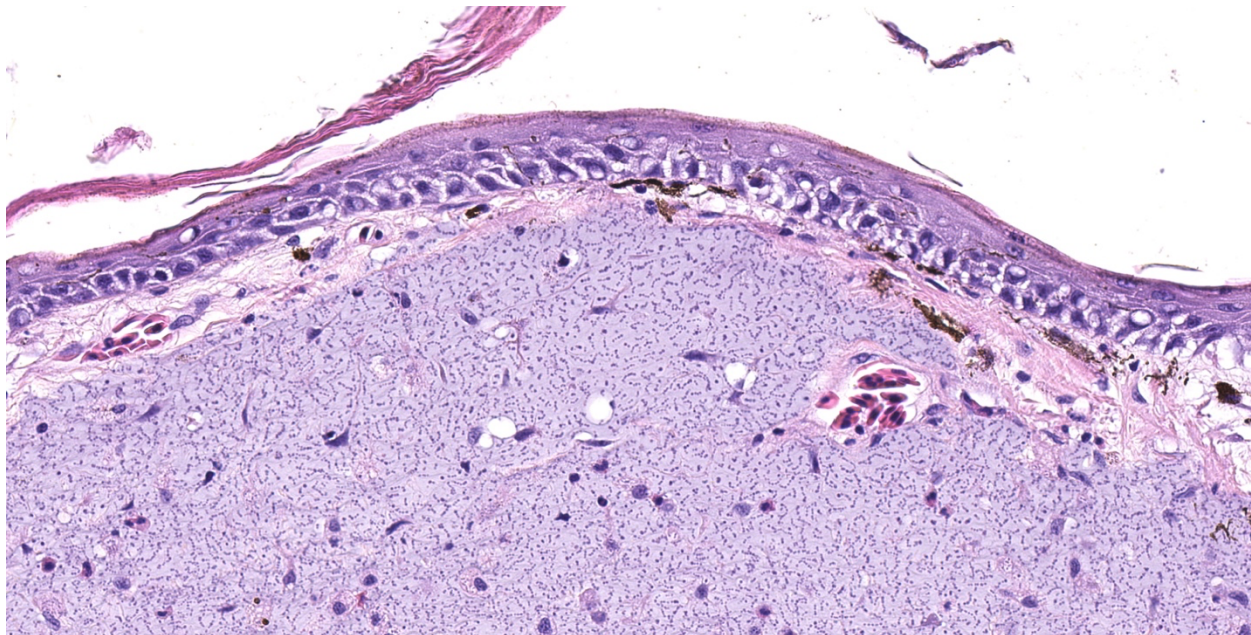
Presentation, brown anole. There are multifocal raised nodules on the tail, limbs and dorsum of this individual. (Photo courtesy of University of Florida College of Veterinary Medicine, Gainesville, FL)



Limb and tail, brown anole. Three sections of limb and tail are submitted for examination. At low magnification, amphiphilic colonies of bacteria elevated the overlying epidermis, and efface the dermis, dermis, skeletal muscle, and bone. (HE, 5X).

linear chains, which are embedded and surrounded by homogeneous, lightly basophilic material. Admixed with the bacteria and sometimes forming a thin rim around the aggregates, there are low to moderate numbers of scattered macrophages, multinucleated giant cells, lymphocytes, and fewer granulocytes. The epidermis overlying the masses ranges from

mildly hyperplastic to multifocally eroded or ulcerated. Areas of ulceration are often covered by a moderately thick crust containing many degenerating granulocytes, sloughed keratin debris, and aggregates of the previously described coccoid bacteria. Skeletal muscle fibers adjacent to the bacterial aggregates sometimes exhibit degenerative changes characterized by myofiber swelling, alterations in staining properties ranging from pallor to hypereosinophilia, fragmentation of the sarcoplasm, and/or nuclear condensation. Aggregates of bacteria multifocally invade and destroy the cortices of vertebral bones, sometimes extending into the spinal canal and wrapping around the spinal cord. Infrequently, a few small aggregates of bacteria with few inflammatory cells are also present within the marrow spaces of vertebrae. The remaining adjacent bone is often irregularly scalloped and exhibits several lightly basophilic reversal lines that parallel the natural margin of the bone. The white matter of the spinal cord contains many empty, dilated axon sheaths, which infrequently contain low numbers of macrophages (digestion chambers). In some, but not all sections, low numbers of nematode larvae are scattered throughout the skeletal muscle, within small cyst-like spaces that are surrounded by a thin rim of



Skin and dermis, brown anole. Numerous curvilinear arrays of encapsulated cocci expand the dermis and elevate the overlying epidermis. (HE, 400X).

epithelioid macrophages and lymphocytes. The nematodes are approximately 80-100 micrometers in diameter, and they have a moderately thick, eosinophilic tegument. They have coelomyarian, polymyarian musculature and prominent lateral cords. There is a central digestive tract lined by several cuboidal to columnar epithelial cells.

Contributor's morphologic diagnosis:

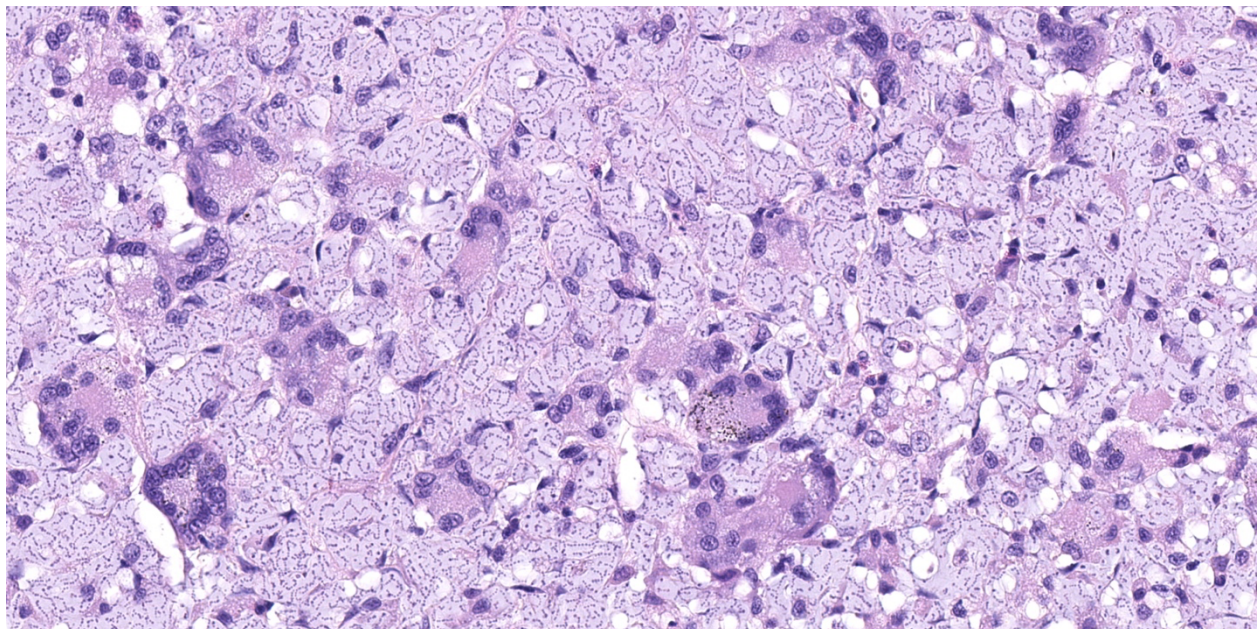
1. Dermatitis, myositis, and osteomyelitis, granulomatous and granulocytic, multifocal to coalescing, chronic, marked, with aggregates of chain-forming, coccoid bacteria and associated myofiber degeneration, bony remodeling, and axonal degeneration
2. Myositis, granulomatous, multifocal, chronic, mild, with intralesional nematode larvae

Contributor's comment:

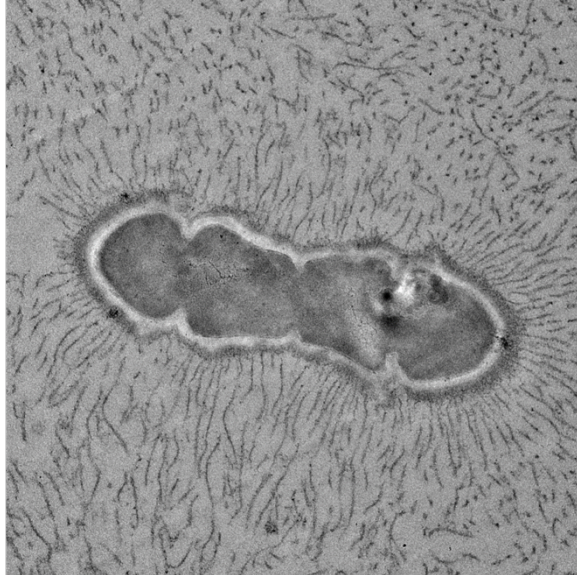
Both the gross and histologic lesions observed in this group of brown anoles exhibited striking similarities to those recently reported in several species of lizards from Christmas Island, an Australian province in the Indian ocean.⁷ Given the morphologic similarities, PCR was performed on a sample obtained from one of the cutaneous

masses, and the resultant gene products revealed 100% sequence identity to the novel *Enterococcus* sp. identified in the lizards from Christmas Island. In both our group of anoles and in all species from Christmas Island (including three species of geckos and one species of skink), the infection was characterized by widespread, multi-organ involvement in which nearly all tissues were multifocally infiltrated and/or partially effaced by similar aggregates of the morphologically distinct bacteria.⁷ Involvement of the head with destruction of mandibular and maxillary bones was a consistent and prominent finding in both groups of lizards.

Rare historical reports of morphologically similar infections have also been documented in several other species of lizards from Malaysia and Germany, although genomic sequencing was not performed in these cases.^{5,10} Despite classification of these organisms as streptococcal species based on morphologic features, the similarity of the histologic lesions and bacterial morphology to the more recent cases suggest that the bacteria may have represented either the same species or a closely related species of *Enterococcus*. In previously reported experimental inoculations, the disease was characterized by high morbidity and mortality



Skeletal muscle and vertebral remnant: Few uni- and multinucleate macrophages are scattered through the bacterial colonies. Rare macrophages contain cytoplasmic melanin granules. (HE, 400X)



500 nm
HV=80.0kV
Direct Mag: 40000x

Skin, brown anole. Bacilli have an undulant thick capsule and numerous fimbriae projecting outward from the surface. (Photo courtesy of University of Florida College of Veterinary Medicine, Gainesville, FL)

and by a slow progression, often taking several months for external lesions to develop and for natural death to ensue.¹⁰ The mechanism of bacterial spread is currently unknown, although the frequency of lesions on the head and jaws has led to speculation that fighting and bite wounds may be involved.¹⁰

The bacteria exhibit distinctive morphologic features and unique staining properties that make them easy to recognize in cytologic or histologic specimens. The organisms form distinct chains and are embedded within a lightly basophilic matrix material. They are gram-positive, although in our experience, the matrix material can interfere with stain uptake, and diastase digestion prior to Gram staining yielded more consistent results. Uniquely, the organisms are also PAS positive, with PAS staining concentrating in a thin rim along the surface of the bacterium. On electron microscopy, the bacteria have a moderately thick capsule and numerous thin, linear structures that project from the surface into the surrounding matrix material, compatible with fimbriae or pili. Despite the markedly high number of bacteria present within lesions, accompanying inflammation is

characteristically mild or sometimes moderate. Presumptively, inflammation may be mitigated by the presence of the thick matrix material in which these organisms are embedded, especially as matrix deposition, the formation of pili, and subsequent biofilm production is a commonly reported contributor to pathogenicity in other species of *Enterococcus*.^{1,7}

In general, *Enterococcus* species are ubiquitous organisms that represent common gastrointestinal commensals of many species, including humans, domestic mammals, and birds.^{1,4} Most frequently, pathogenicity is associated with opportunistic infections, and multi-drug resistance is commonly reported in both humans and veterinary species.^{1,4} *Enterococcus* sp. are fastidious organisms and often require specific media conditions for successful growth in culture.⁷

Although not present in all submitted slides, many of the slides included one or more sections of intramuscular nematode larvae within thin-walled granulomas. These organisms were considered incidental and likely unrelated to the systemic *Enterococcus* sp. infection.

Contributing Institution:

University of Florida College of Veterinary Medicine

Department of Comparative, Diagnostic, and Population Medicine

<https://cdpm.vetmed.ufl.edu/>

JPC diagnosis:

1. Limbs and tail, dermis, skeletal muscle, bone: Large colonies of cocci with mild lymphoplasmacytic and histiocytic dermatitis, brown anole, lizard.
2. Limb: Granulomas, multiple, with nematode larvae.

JPC comment:

During conference discussion, it was noted that some sections and slides may not have contained nematode larvae within granulomas. However, a short discussion of anatomic and morphologic features of nematodes and their larvae took place.

The contributor concisely describes *Enterococcus* infections across several species. Much of the body of knowledge about *Enterococcus* species has been built from research on *E. faecalis* and *E. faecium*, pathogens that produce disease in humans. Features that contribute to virulence and pathogenicity include aggregation substance (an adhesin), a capsule, the cell wall, pili, cytolysin, secretion of extracellular superoxide, gelatinase, iron acquisition, enterococcal surface protein (*esp*), and a variety of microbial surface components recognizing adhesive matrix molecules (MSCRAMMs).⁸

Enterococcus faecium, though a normal commensal of the human gastrointestinal tract, is a frequent cause of septicemia in hospitalized patients. Using transcriptome profiling (RNA-seq) and high-throughput transposon mutant library sequencing (Tn-seq) to evaluate a vancomycin-resistant clinical isolate, specific genes were identified that allowed for survival and exponential growth in human serum. Several genes involved in de novo nucleotide biosynthesis (*pyrK_2*, *pyrF*, *purD*, and *purH*) and carbohydrate uptake (*manZ_3*, *manY_2*, *ptsL*) conferred the greatest virulence, and were critical to growth in serum.⁹

In poultry, *Enterococcus cecorum* infection has been documented extensively, worldwide, since its first description in 1983. While this disease is notable for causing skeletal disease in broiler and broiler breeder chickens, the most striking feature is paralysis caused by an inflammatory mass that develops in the spinal column. This usually results in the bird sitting with both legs extended cranially and is considered a classic symptom.³

Other reported infections in the brown anole also include Ranavirus (OIE reportable in amphibians but not reptiles), reovirus, and fungi of the *Chrysosporium anamorph* of *Nannizziopsis vriesii*-complex (CANV-complex).⁶

A feature unique to some species of Lacertilia that has spurred research involves fracture planes and regrowth of lost tails. Though it lacks normal structure and is paler, muscle is regenerated, along with a cartilaginous tube in place of true vertebra.⁶ The key feature that allows

regeneration is the blastema formation at the site of detachment, an aggregate of proliferating cells under a new, scar-free, epithelial layer. The cells of the blastema differentiate into all regenerated tissue types, though is likely lineage-restricted to one germ layer. While there are variations in regeneration of axolotls, salamanders, telosts, and lizards, current evidence indicates that ependymal cells of the spinal cord are most critical to the coordinated growth and differentiation of the blastema. With lizards the closest living relatives to mammals that are capable of scar-free healing, they have become the animal model for regenerative research in humans.²

References:

1. Arias CA, Murray BE. The rise of the *Enterococcus*: beyond vancomycin resistance. *Nat Rev Microbiol.* 2012;10: 266-278.
2. Gilbert EAB, Delorme SL, Vickaryous MK. The regeneration blastema of lizards: an amniote model of the study of appendage replacement. *Regeneration.* 2015;2(2):45-53.
3. Jung A, Chen LR, Suyemoto MM, Barnes HJ, Borst LB. A review of *Enterococcus cecorum* infection in poultry. *Avian Diseases.* 2018;62:261-271.
4. Kataoka Y, Umino Y, Ochi H, Harada K, Sawada T. Antimicrobial susceptibility of enterococcal species isolated from antibiotic-treated dogs and cats. *J Vet Med Sci.* 2014;76: 1399-1402.
5. McNamara TS, Gardiner C, Harris RK, Hadfield TL, Behler JL. Streptococcal Bacteremia in Two Singapore House Geckos (*Gekko monarchus*). *Journal of Zoo and Wildlife Medicine.* 1994;25: 161-166.
6. Origgi FC. Lacertilia. In: Terio KA, McAloose D, St. Leger J, ed. *Pathology of Wildlife and Zoo Animals.* San Diego, CA: Elsevier. 2018:871-887.
7. Rose K, Agius J, Hall J, et al. Emergent multisystemic *Enterococcus* infection threatens endangered Christmas Island reptile populations. *PLoS One.* 2017;12: e0181240.
8. Stewart Gc. *Streptococcus* and *Enterococcus*. In: McVey DS, Kennedy M, Shengappa MM eds. *Veterinary Microbiology.* Ames, IA: Wiley-Blackwell. 2013:199-201.
9. Zhang X, de Matt V, Prieto AMG, et al. RNA-seq and Tn-seq reveal fitness

determinants of vancomycin-resistant *Enterococcus faecium* during growth in human serum. *BMC Genomics*. 2017;18:893.

10. Zwart P: Streptokokkensepsis mit Hautwucherungen bei Eidechsen. International Conference of Zoo Animal Diseases, 1972

CASE 2: F930 VP19265N (4152714-00)

Signalment:

1-year 6-months-old, female, African hedgehog (*Atelerix albiventris*)

History:

The hedgehog showed ataxia and visited the animal hospital. At the time of the initial visit, the hedgehog was mildly thin and showed ataxia in the bilateral forelimb. Although corticosteroid, vitamin B complex, and vitamin E were continuously administered, the symptoms progressed to paralysis, and the hedgehog was died two months later.

Gross Pathology:

At necropsy, 3.5 mm soft, gelatinous, and grayish white mass was formed in rostral end of the right cerebral hemisphere. The liver was enlarged and discolored, and pulmonary edema was observed.

Laboratory results:

There were no abnormal findings on CBC, serum chemistry analysis, abdominal ultrasonography, and chest X-ray.

Microscopic description:

In the rostral end of the cerebrum, there is a well-demarcated, unencapsulated mass. The neoplasm is composed of diffusely growing round to angular cells. Neoplastic cells are 10-18 microns in diameter with glassy, abundant eosinophilic cytoplasm and have distinct cell borders. Nuclei are round to oval and eccentric, with finely stippled chromatin and indistinct nucleoli. Mitotic figures are rare. The neoplastic cells stained positively for GFAP, but negative with Olig2 and Iba-1.

Contributor's morphologic diagnosis:

Brain (cerebrum): Gemistocytic astrocytoma.

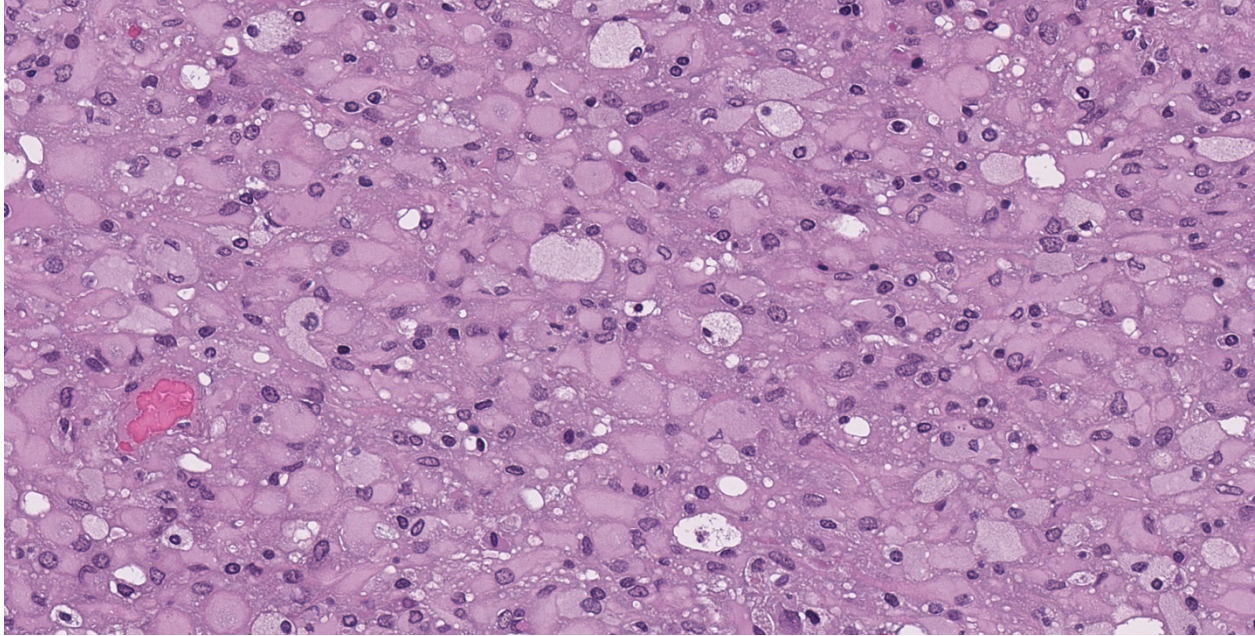
Contributor's comment:

Astrocytomas are a type of glioma that consist of neoplastic cells that are morphologically similar to astrocytes and occurs in the brain and spinal cord. This tumor is well known in dogs and is divided into three grades by World Health Organization (WHO) classification on tumors of domestic animals: low-grade (well-differentiated), medium-grade (anaplastic), and high-grade (glioblastoma) astrocytomas.⁵ Additionally, low-grade astrocytomas are classified into three subtypes: fibrillary, protoplasmic, and gemistocytic astrocytoma.⁵ Our case consistent with gemistocytic astrocytoma in terms of large, round to angular neoplastic cells with abundant eosinophilic cytoplasm.

In African hedgehogs, astrocytoma, oligodendroglioma, oligoastrocytoma, ganglioglioma, and histiocytic sarcoma have been reported as primary intracranial tumors.^{1,3,8-10} Muñoz-Gutiérrez et al. reported a series of primary central nervous system neoplasms in African hedgehogs, with primary central nervous system neoplasms identified in 12 of 762 hedgehogs.⁸ Of the 12 cases in their report, six were gangliogliomas, five were astrocytomas, and one was an oligodendroglioma, and all astrocytomas were gemistocytic subtype.⁸ Additionally, two cases of anaplastic astrocytoma have been reported.^{3,9}



Cerebrum, hedgehog. A nodular, well-demarcated neoplasm effaces 33% of the section of cerebrum. (HE, 5X)



Cerebrum, hedgehog. Sheets of neoplastic astrocytes separated by small amounts of vacuolated parenchyma comprise the neoplasm. The neoplastic cells have abundant eosinophilic cytoplasm and resemble gemistocytic astrocytes. As neoplastic cells undergo degeneration, they become swollen, vacuolated and have hyperchromatic nuclei. (HE, 395X)

Clinical symptoms such as progressive ataxia and paralysis suggestive of central nervous system manifestation should be differentiated from wobbly hedgehog syndrome (WHS) in African hedgehog. Histopathologically, WHS is characterized by bilaterally symmetrical myelin degeneration in the white matter.² In our case, the onset of symptoms was at a young age of less than 2 years of age, and WHS was clinically suspected. However, WHS was clearly denied by confirmed the neoplastic lesion and the absence of myelin degeneration. Because some primary intracranial tumors do not form clear masses, a detailed pathological observation of the brain and spinal cord is needed to rule out WHS.

Contributing Institution:

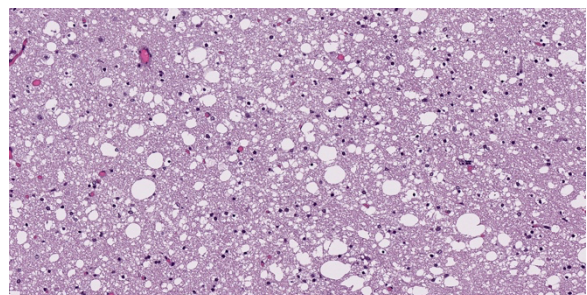
Laboratory of Pathology
 Faculty of Pharmaceutical Sciences
 Setsunan University
 45-1 Nagaotohge-cho, Hirakata
 Osaka 573-0101, Japan

JPC diagnosis:

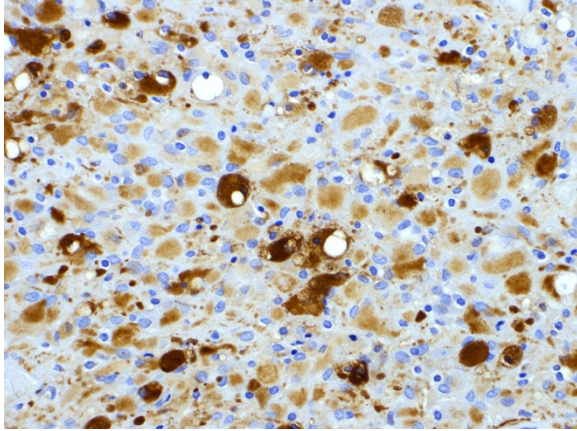
Cerebrum: Gemistocytic astrocytoma, low grade, African hedgehog, Erinaceinae.

JPC comment:

The contributor provides a brief summary of astrocytomas and Wobbly Hedgehog Syndrome. The 2016 WHO classification for human astrocytic neoplasms differs from the reference WHO classification in domestic animals, and now all diffuse human gliomas (astrocytic and not) are grouped together based on growth patterns and behaviors, and also the shared mutated isocitrate dehydrogenase (*IDH*) gene status. The new classification category includes WHO grade II and III astrocytic tumors, grade II and III oligodendrogliomas, grade II and III oligoastrocytomas, grade IV glioblastomas, and diffuse gliomas of childhood. While occasional gemistocytic astrocytes would be considered



Cerebrum, hedgehog. There is marked spongiosis, dilated axon sheaths, and mild gliosis of the surrounding parenchyma. (HE, 400X)



Cerebrum, hedgehog. The cytoplasm of large polygonal (gemistocytic) neoplastic astrocytes stain strongly and diffusely with an antibody against glial fibrillary astrocytic protein. (ant-GFAP, 400X). (Photo courtesy of Laboratory of Pathology, Faculty of Pharmaceutical Sciences, Setsunan University, 45-1 Nagaotoge-cho, Hirakata, Osaka 573-0101, Japan)

normal in a diffuse astrocytoma, there must be more than 20% gemistocytic astrocytes for the diagnosis of gemistocytic astrocytoma. As in this case, gemistocytic astrocytoma cells demonstrate strong cytoplasmic immunoreactivity to GFAP, and more than 80% of (human) cases exhibit nuclear immunoreactivity to p53.⁷

IDH mutation status provides important diagnostic and prognostic information for patients with diffuse gliomas. IDH status may also be associated with efficacy of individualized treatment, therapeutic vaccines, and anti-IDH treatment. While the gold standard for diagnosis of IDH status is immunohistochemistry (R132H antibody), recent computational pathology efforts have focused on making IDH status determination using H&E slides only. Deep learning models were developed using a training set of known IDH-mutated and IDH-wild type cases, and further augmented by Generative Adversarial Network (GAN) training, resulting in an accuracy of classification by IDH status of 85% using H&E alone. Adding an age variable to the model (< 55 years of age, 55 years of age or older) further improved the accuracy of classification to 96% in the older age group. This category of computational pathology may someday improve medical care and efficiency of resources.⁶

GFAP is usually considered a well conserved intermediate filament expressed in well differentiated, less malignant astrocytic neoplasms. However, GFAP expression has also recently been observed in radial glia of the developing (human) brain, and in adult neural stem cells, indicating the GFAP is also expressed in immature, less fully differentiated glial cells. While GFAP expression may not be correlated with astrocytoma of different grades of malignancy, the two isoforms of GFAP may be useful markers for this determination. Higher levels of GFAP δ expression (alternative splice variant) relative to the normal isoform GFAP α appears to be correlated with higher grades of malignancy. Further research in veterinary species may be warranted in light of this human-centric work.¹²

The recently revised classification of canine gliomas attempts to simplify the categorization of these neoplasms and does not rely on stratification based on mutational status of previously identified susceptible genes in humans.⁴ While a very small sample size, it was once found that none of 25 sampled canine gliomas contained an IDH mutation, suggesting a potentially different pathogenesis than human gliomas.¹¹ However, as was stated in the revised classification, "there is much to learn about the histogenesis and behavior of these tumors ... a more detailed system will depend on future molecular studies and more thorough clinical annotation."⁴

References:

1. Benneter SS, Summers BA, Schulz-Schaeffer WJ, Härtig W, Mollidor J, Schöniger S. Mixed Glioma (Oligoastrocytoma) in the brain of an African hedgehog (*Atelerix albiventris*). *J Comp Pathol.* 2014;151:420–424.
2. Díaz-Delgado J, Whitley DB, Storts RW, Heatley JJ, Hoppes 3, Porter BF. The Pathology of wobbly hedgehog syndrome. *Vet Pathol.* 2018;55:711–718.
3. Gibson CJ, Parry NM, Jakowski RM, Eshar D. Anaplastic astrocytoma in the spinal cord of an African pygmy hedgehog (*Atelerix albiventris*). *Vet Pathol.* 2008;45:934–938.
4. Koehler JW, Miller AD, Miller CR, et al. A revised diagnostic classification of canine

glioma: towards validation of the canine glioma patient as a naturally occurring preclinical model for human glioma. *J Neuropathol Exp Neurol.* 2018;77(11):1039-1054.

5. Koestner A, Bilzer T, Fatzer R, Schulman FY, Summers BA, Van Winkle TJ: Astrocytic tumors. In: Histological classification of tumors of the nervous system of domestic animals, pp. 17–19. World Health Organization, Washington, DC, 1999.
6. Liu S, Shah Z, Sav A, et al. Isocitrate dehydrogenase (IDH) status prediction in histopathology images of gliomas using deep learning. *Sci Rep.* 10, 7733 (2020).
7. Louis DN, von Deimling A, Cavenee WK. Diffuse astrocytic and oligodendroglial tumours - Introduction. In: *WHO Classification of Tumours of the Central Nervous System.* Lyon, France: International Agency for Research on Cancer. 2016:15-23.
8. Muñoz-Gutiérrez JF, Garner MM, Kiupel M. Primary central nervous system neoplasms in African hedgehogs. *J Vet Diagn Invest.* 2018;30:715–720.
9. Nakata M, Miwa Y, Itou T, Uchida K, Nakayama H, Sakai T. Astrocytoma in an African hedgehog (*Atelerix albiventris*) suspected wobbly hedgehog syndrome. *J Vet Med Sci.* 2011;95:255–257.
10. Ogihara K, Suzuki K, Madarame H. Primary histiocytic sarcoma of the brain in an African hedgehog (*Atelerix albiventris*). *J Comp Pathol.* 2017;157:241–245.
11. Reitman ZJ, Olby NJ, Mariani CL, et al. IDH1 and IDH2 hotspot mutations are not found in canine glioma. *Int J Cancer.* 2010;127(1):245-246.
12. Van Bodegraven EJ, van Asperen JV, Robe PAJ, Hol EM. Importance of GFAP isoform-specific analysis in astrocytoma. *Glia.* 2019;67:1417-1433.

CASE 3: 19080625 (4152936-00)

Signalment:

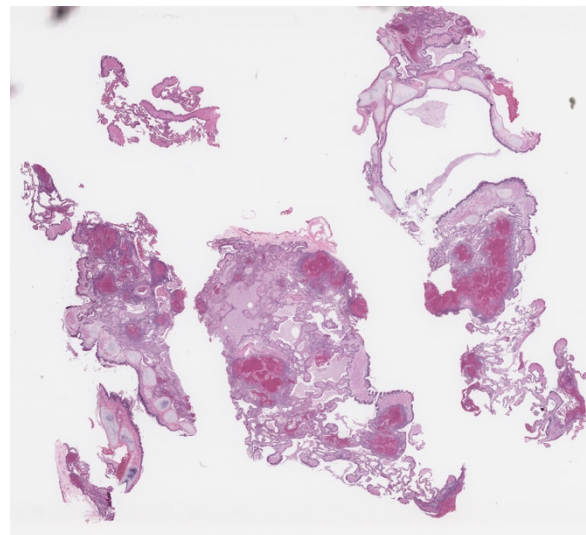
A 7-year-old, intact female, leopard tortoise (*Stigmochelys pardalis*)

History:

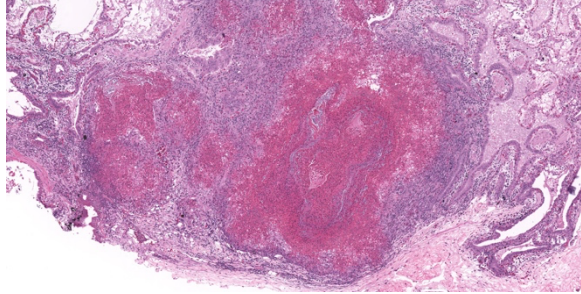
This animal had a one-month history of respiratory distress and nasal discharge.

Gross Pathology:

The oral cavity contains multiple off-white to light tan, confluent plaques on the lingual and gingival mucosa. Numerous, viable, beige, cylindrical, approximately 0.3 to 0.4 cm diameter ectoparasites (fly larvae) infiltrate the esophageal and peri-esophageal soft tissues at the entry of the esophageal tube. A red, 0.5 cm diameter, skin discoloration is present under the chin. The caudal coastal and vertebral carapaces are raised. Multiple cystic spaces, measuring up to 1-1.5 cm diameter, are observed in the left lung. These cystic structures are filled with a moderate amount of yellow-tan, clear and mucoid fluid. Numerous, up to 1 mm diameter, pale tan to white foci are evident on the surfaces of the spleen and liver. On cut section, these foci are scattered throughout the splenic and hepatic parenchyma. The stomach contains approximately 100 mLs of grey to brown, mucoid fluid. Two pale, raised, pinpoint foci are present on the mucosal surface of the stomach. The intestinal lumen contains a mixture of tan to pink, semisolid ingesta. Formed, dark green feces are present in the distal colon.



Lung, leopard tortoise. Multiple sections of lung are submitted for examination. At low magnification, there is multifocal consolidation with numerous brightly eosinophilic aggregates of heterophils. (HE, 5X)



Lung, leopard tortoise. Higher magnification of the heterophilic and granulomatous inflammation effacing the faveolar septa and filling faveolar air spaces. (HE, 53X)

Laboratory results:

Aerobic culture of the lung yielded large numbers of *Proteus* spp., *Enterococcus faecalis*, *Alcaligenes* spp., *Citrobacter braakii*, and moderate numbers of *Pseudomonas aeruginosa*, *Escherichia coli*, *Providencia* spp., *Enterococcus casseliflavus*, and *Morganella morganii*

Microscopic description:

Lung: Moderately to markedly filling random bronchi and bronchioles, also with multifocal expansion of the interstitium, are multifocal to coalescing areas of necrosis, composed of massive amounts of cellular and nuclear debris, numerous degenerate heterophils, and myriad numbers of intralesional coccobacilli. Necrotic foci are sometimes surrounded by increased numbers of intact heterophils and fewer macrophages. Affected bronchi and bronchioles are lined by either intact and necrotic, or absent epithelium. In other less affected areas, the bronchial and bronchiolar epithelium remains intact, and is moderately to markedly hyperplastic, with occasional intranuclear protozoa at various stages of development (coccidia). Developmental stages present include: intranuclear ovoid to spherical gametes that are up to 5-6 μm in diameter with granular basophilic cytoplasm and eccentric nucleus; intranuclear spherical meronts that are 5-7 μm with numerous banana-shaped merozoites; and intraluminal unsporulated oocysts that are approximately 8-12 μm in diameter. Multifocally, ectatic respiratory lumina often contain slightly granular, proteinaceous cellular debris interspersed with coccidia at various stages of development.

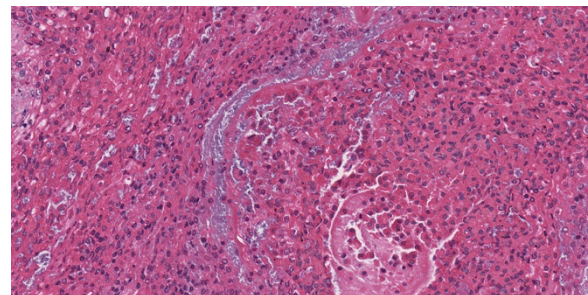
Contributor's morphologic diagnosis:

Lung: Bronchointerstitial pneumonia, necrotizing, heterophilic and histiocytic, subacute, multifocal to coalescing, marked, with bronchi and bronchiolar epithelial hyperplasia with intranuclear protozoal coccidia, and intralesional coccobacilli

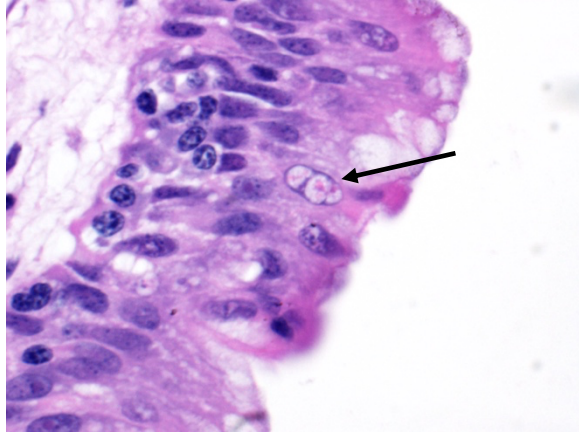
Contributor's comment:

The microscopic features of the lung are consistent with the entity described as Intranuclear coccidiosis of testudines (TINC), which is presumed to be the primary change in this case. A variety of bacteria were isolated from the lung but are likely resultant from opportunistic infection or environmental contaminants.

Infection of Testudines with intranuclear coccidia was first identified in the 1990s, and has now emerged as one of the most important infectious diseases affecting a variety of chelonian species.^{4,7} Reported species to date include radiated tortoise (*Geochelone radiata*), impressed tortoise (*Manouria impressa*), leopard tortoise (*Geochelone pardalis*), Travancore tortoise (*Indotestudo forstenii*), Bowsprit tortoise (*Chersine angulate*), Sulawesi tortoise (*Indotestudo forsteni*), Eastern box turtle (*Terrapene carolina*), Arakan forest turtles (*Heosemys depressa*), Spider tortoise (*Pyxis arachnoides*), flat-tailed tortoises (*Pyxis planicauda*), Galapagos tortoises (*Chelonoidis nigra becki*), marginated tortoise (*Testudo marginata*), Hermann's tortoise (*Testudo hermanni*), Greek tortoise (*Testudo graeca*), Russian tortoise (*Testudo horsfieldi*), Indian star tortoise, African spurred tortoise (*Geochelone*



Lung, leopard tortoise. Heterophilic inflammation is often centered on bacterial colonies. (HE, 400X)



Lung, leopard tortoise. Scattered throughout the section are areas in which faveolar pneumocytes contain developing intranuclear coccidial gamonts. (HE, 400X)

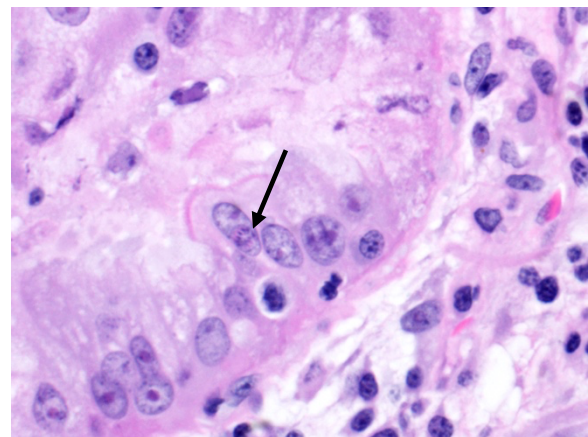
sulcata), and yellow footed tortoise (*Chelonoidis denticulatus*).^{2,3,5-8} The causative agent of TINC is a novel coccidia that has not been assigned to a genus as of yet; however, the 18S ribosomal RNA (rRNA) nucleotide sequencing analysis reveals that it is most closely related to *Eimeria arnyi* and *Eimeriid coccidium*, based on two separate studies.^{5,6}

The route of transmission of TINC remains elusive, but direct, fecal-oral transmission is most likely, based on the finding of oocysts in the feces of TINC-positive tortoises, and successful infection of other tortoises following experimental oral inoculation.⁵ The unsporulated oocyst of this parasite is spherical, and measures 6-12 μm in diameter with a centrally located sporont.^{5,7} Sporulation of the oocysts requires 3-4 days, which is a crucial stage during the life cycle of TINC.⁵ The sporulated oocyst contains four sporocysts, which are thin and smooth walled, surrounding two sporozoites.⁵ Within the infected mammalian cell nuclei, one or more coccidia at variable stages of development can be detected. Trophozoites measure 2-5 μm in diameter.^{3,6} Meronts are up to 7 μm in diameter with numerous merozoites.^{3,6} Merozoites are banana shaped, and measure 4 X 1.5 μm with a single central to slightly³⁻⁷ eccentric nucleus.^{3,6} Macrogametes and microgametes are spherical and up to 6 μm in diameter.^{3,6}

Clinical signs can be variable and include: anorexia, lethargy, weight loss, weakness,

increased respiratory effort, mild chronic conjunctival erythema, bilateral ocular and nasal mucoid discharges, oronasal fistula, ascites, retained urine in the urinary bladder, severe cutaneous edema and/or ulceration.^{3,4,6,8} Death can occur within a few days after initial onset of clinical signs of disease.^{3,4} Useful antemortem diagnostic methods include cytologic examination of the nasal discharge, histologic examination of the affected tissue via biopsy, and molecular testing such as polymerase chain reaction (PCR) performed on swab specimens from the oral, ocular, nasal, and cloacal mucosa.^{4,6} Cytologic preparations generally include a predominance of lymphocytes and plasma cells, with fewer macrophages and granulocytes. Intranuclear coccidia can sometimes be detected within affected epithelia stained with Fite acid-fast, Periodic Acid-Schiff (PAS), or Wright-Giemsa.⁶

TINC is a systemic disease, and gross lesions can be observed within a diversity of organ systems to include: alimentary, respiratory, cardiovascular, urogenital, and integumentary.³⁻⁷ The common gross findings include pallor of mucous membranes, thick oral mucus, pseudomembranous enteritis, cloaca erythema, rhinitis, pulmonary congestion, pericardial and intestinal petechiae, firm kidneys with a gray to red mottled discoloration, splenic congestion, discolored liver, distended urinary bladder, and generalized subcutaneous edema.³⁻⁷ Histologically, lymphoplasmacytic inflammation and necrosis with intranuclear, or less frequently,



Lung, leopard tortoise. Multiple intranuclear zoites within schizonts are found within affected faveolar pneumocytes. (HE, 400X)

intracytoplasmic and extracellular coccidial organisms are evident within the affected tissue.^{3,4,6,7} Various stages of coccidia are more commonly seen in the nucleus of respiratory epithelium, hepatocytes, biliary tree epithelium, pancreatic ductular and acinar cells, enterocytes, renal tubular epithelium, and urinary bladder epithelium, but they can also be detected in thyroid and adrenal glands, gonads, lymphoid organs, and skin.^{3,4,6,7} Quantitative PCR (qPCR) is a rapid and sensitive diagnostic option for confirmation of TINC in suspected cases.²

Contributing Institution:

Department of Veterinary Pathobiology
College of Veterinary Medicine
Oklahoma State University
<https://vetmed.okstate.edu/veterinary-pathobiology/index.html>

JPC diagnosis:

1. Lung: Pneumonia, interstitial, granulocytic, histiocytic, with bacterial colonies, type II pneumocyte hyperplasia, and interstitial fibrosis, leopard tortoise, chelonid.
2. Lung, bronchiolar and faveolar epithelium: Hyperplasia and lymphocytic inflammation, with intranuclear gamonts, intranuclear meronts, intracytoplasmic zoidites, and extracellular oocysts.

JPC comment:

The concurrent bacterial pneumonia in this case likely contributed significantly to clinical signs. The inflammation is primarily centered on faveoli, indicating a likely hematogenous route of entry to the lungs. If the described lesions in the spleen and liver are similar in character to those in the lung, this animal was likely septic. However, without sections of other tissues, a definitive diagnosis can only be speculative.

The contributor provides an excellent summary of this emerging disease of testudines. Since submission, this unnamed coccidian has also been documented in the red-footed tortoise (*Chelonoidis carbonaria*). One interesting aspect of this disease is that all discovered cases have occurred in managed-care settings, to include

recently imported animals. With no documented cases in wild chelonians, there may be either too few free-living chelonian cases investigated^{1,11}, and/or there is a variable related to captivity that modulates disease in these animals.

Current recommended therapy includes antiparasitic medications, such as toltrazuril or ponazuril, though care should be taken not to conclude treatment prematurely. Chelonians that die following treatment have had fibrosis in areas previously infected by the apicomplexan, illustrating its potential long-term tissue damage to organs.¹

Tortoises often enjoy a long life but remain susceptible to environmental changes. Lonesome George was the ending Pinta Island tortoise (*Chelonoidis abingdonii*), and lived on Pinta Island, a small island of the Galapagos Islands chain, of Ecuador. Discovered in 1971, he remained the last tortoise in the face of environmental degradation from introduced feral goats. He was relocated to the Charles Darwin Research Station on a nearby island for his safety, but never successfully reproduced with females of closely related species. He died in 2012, an estimated 100 years old, still thought to be relatively young for a tortoise of his species.¹⁰

Giant tortoises are among the longest-lived vertebrates and are studied as models of longevity and age-related disease. A global genetic analysis was performed on Lonesome George following his death. For comparison, a genome of *Aldabrachelys gigantea* was also sequenced, as a related tortoise that diverged from *Chelonoidis abingdonii* approximately 40 million years ago. Across a number of genes, there were similar numbers of copies of tumor suppressor genes (*PTPN11*, *P2RY8*, *PML*, *NF2*, *SMAD4*, *PRDM1*) in these two tortoise species, and there were more copies than in the human genome. Similarly, across several genes associated with ageing (*NEIL1*, *RMI2*, *EEF1A1*, *GAPDH*), the tortoises' genomes had more copies of genes than the human genome, most of which contribute to DNA stability and result in fewer mutations over time. Continued research with these genomes may reveal novel therapeutics or interventions to increase human survival with increased health.⁹

References:

1. Adamovicz L, Allender MC, Gibbons PM. Emerging Infectious Disease of Chelonians: An Update. *Vet Clin Exot Anim.* 2020;23:263-283.
2. Alvarez WA, Gibbons PM, Rivera S, Archer LL, Childress AL, Wellehan JFX. Development of a quantitative PCR for rapid and sensitive diagnosis of an intranuclear coccidian parasite in Testudines (TINC), and detection in the critically endangered Arakan forest turtle (*Heosemys depressa*). *Vet Parasitol.* 2013;193:66–70.
3. Garner MM, Gardiner CH, Wellehan JFX, et al. Intranuclear coccidiosis in tortoises: Nine cases. *Vet Pathol.* 2006;43:311–320.
4. Gibbons PM, Steffes ZJ. Emerging Infectious Diseases of Chelonians. *Vet Clin North Am - Exot Anim Pract.* 2013;16:303–317.
5. Hofmannová L, Kvičerová J, Bízková K, Modrý D. Intranuclear coccidiosis in tortoises — discovery of its causative agent and transmission. *Eur J Protistol.* 2019;67:71–76.
6. Innis CJ, Garner MM, Johnson AJ, et al. Antemortem diagnosis and characterization of nasal intranuclear coccidiosis in Sulawesi tortoises (*Indotestudo forsteni*). *J Vet Diagnostic Investig.* 2007;19:660–667.
7. Jacobson ER, Schumacher J, Telford SR, Greiner EC, Buergelt CD, Gardiner CH. Case report of systemic coccidiosis in a radiated tortoise (*Geochelone radiata*). *J Zoo Wildl Med.* 1994;25:95–102.
8. Kolesnik E, Dietz J, Heckers KO, Marschang RE. Detection of Intranuclear Coccidiosis in Tortoises in Europe and China. *J Zoo Wildl Med.* 2017;48:328–334.
9. Quesada V, Freitas-Rodriguez S, Miller J, et al. Giant tortoise genomes provide insights into longevity and age-related disease. *Nature Ecology and Evolution.* 2019;3:87-95.
10. Raferty, Isolde. "Lonesome George, last-of-its-kind Galapagos tortoise, dies". MSNBC. Archived from the original on 2012-06-27. Retrieved 2020-08-23.
11. Rodriguez CE, Duque AMH, Steinberg J, Woodburn DB. Chelonia. In: eds Terio KA, McAloose D, St. Leger, J. *Pathology of Wildlife and Zoo Animals.* San Diego, CA:Elsevier. 2018:847:848.

CASE 4: D18-10210 (4135869-00)

Signalment:

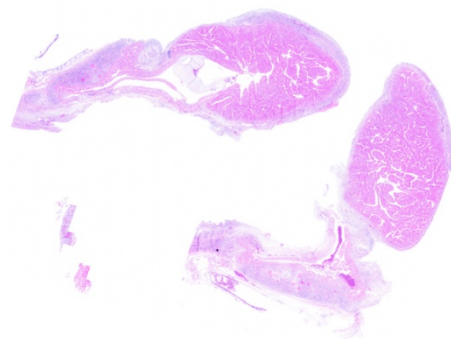
6-month-old, male intact inland bearded dragon (*Pogona vitticeps*)

History:

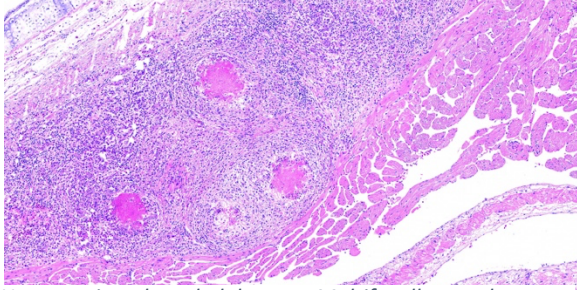
The animal had a 5-d course of anorexia and lethargy with terminal right head tilt. The animal was fed a daily diet of 10–15 superworms (commercially purchased), green turnips, and collard greens. The animal died 1 d after the owner noted that the beard of the animal had turned black.

Gross Pathology:

The animal was in a good nutritional state, weighing 145 g. The pericardial sac was markedly dilated and filled with clotted and unclotted blood. Fibrinous exudate adhered to and diffusely coated the inner aspect of the pericardial sac. Poorly defined white homogeneous glossy tissue was present at the base of the heart. The heart was maximally contracted. The coelomic cavity contained ~4 mL of clear amber watery fluid (hydrocoelom). An ~1 × 1.3 cm diameter conglomerate of ~0.5 cm diameter, smooth, beige nodules was present next to both testes.



Heart, bearded dragon. Two sections of the heart are presented for examination. The ventricle and atrial appendage are covered by a thick layer of cellular fibrous connective tissue. (HE, 5X)



Heart, atrium, bearded dragon. Multifocally, poorly formed heterophilic granulomas are scattered through the markedly thickened epicardium. (HE, 75X)

Laboratory results:

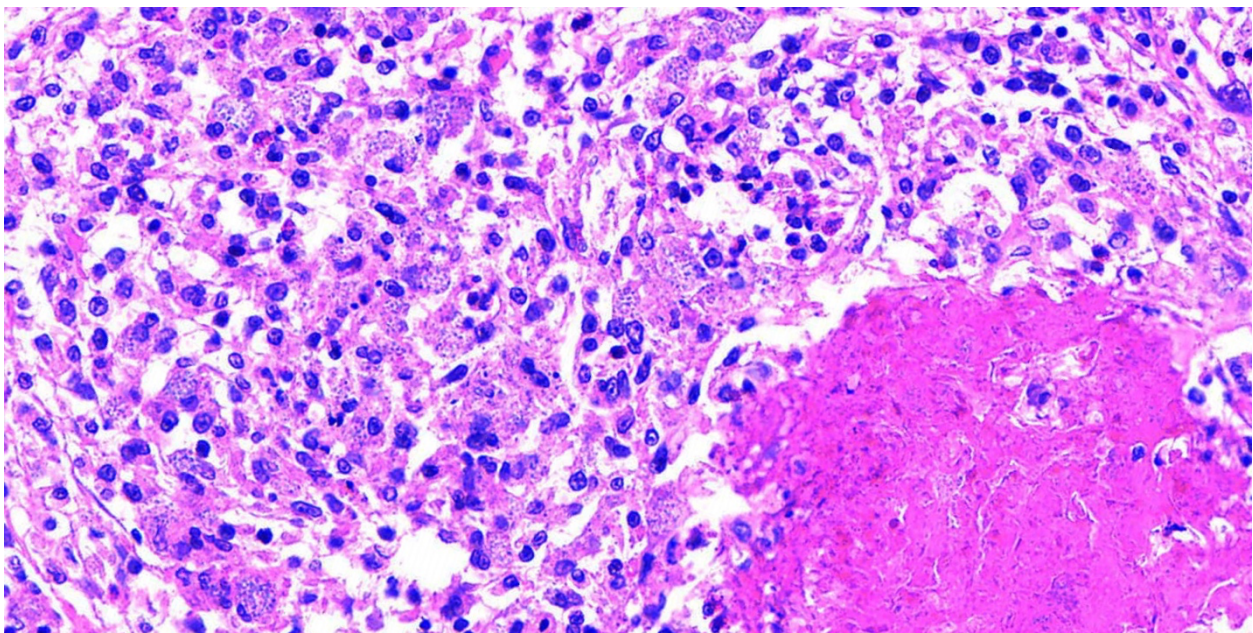
A 265-bp sequence of the internal transcribed spacer 1 (ITS1) region of the ribosomal RNA gene was 100% homologous with *E. pogonae* (GenBank accession KR998311).

Microscopic description:

The slide contained a longitudinal section of the heart with the ventricle and one atrium. The epicardial surface of the atrium was expanded and covered by a densely cellular infiltrate largely composed of macrophages admixed with fewer heterophilic granulocytes. Multifocally within the atrial epicardial infiltrate, epithelioid macrophages were arranged around a core of eosinophilic debris. This debris contained numerous, weakly basophilic-staining

microorganisms. These microorganisms were slightly elongated, up to 2 μm long, and contained a vacuole. The cytoplasm of occasional macrophages was extended by similar microorganisms. The organisms were gram-positive and weakly PAS-positive but acid-fast-negative and negative with the GMS stain. Giemsa stain highlighted the wall and nucleus of the microorganisms. The epicardium of the ventricle and of one atrium (of the heart) were multifocally lined by a thick membrane of fibrous connective tissue. The connective tissue membrane covering the ventricle contained scattered mixed cellular inflammatory infiltrates (lymphocytes, plasma cells, macrophages and heterophilic granulocytes). The fibrous connective membrane covering the apex of the heart had subtle fibrin deposits on the outer surface.

On transmission electron microscopy, the microorganisms were identified as microsporidians based on the presence of exospore, endospore, vacuole, nucleus, and a polar filament. The organisms averaged 1.83 μm long \times 0.92 μm wide. The polar filaments had 4–6 coils and averaged 61 nm in diameter.



Heart, atrium, bearded dragon. At the periphery of the heterophilic granulomas, macrophages contain numerous 2-3um microsporidial spores in their cytoplasm. (HE, 554X)

Contributor's morphologic diagnosis:

Heart, epicarditis, granulomatous and heterophilic, widespread, chronic, marked with intrahistiocytic microorganisms (presumably microsporidia)

Contributor's comment:

The contributor writes in his most recent journal article on this subject:

"Microsporidia are atypical fungi that parasitize and cause disease in invertebrates, fish, amphibians, reptiles, and mammals.¹⁹ Microsporidia reproduce within the host cell, including macrophages, in which they are detectable histologically.^{3,18} The spores are oblong and have a clear vacuole. They measure up to 3 µm long and ~1 µm in diameter, although some species have larger spores.¹ Mature spores are refractile, gram-positive, and have variable tinctorial properties when stained with silver stains, Giemsa stain, and when subjected to the PAS reaction.³ On electron microscopy, the spores are characterized by an exospore, endospore, and coiled polar tubular filament.^{9,11} The number of windings of this filament varies depending on species and developmental stage. Fatal and non-fatal microsporidian infections have been reported in central bearded dragons (syn. inland bearded dragon; *Pogona vitticeps*).^{6,10,12,14,15} In 2016, a microsporidian detected in a bearded dragon was identified as the new species *Encephalitozoon pogonae*.^{15"}

The case presented was characterized by a cardiac manifestation that led to hemopericardium presumably as a result of hemorrhage from the granulation tissue and likely to an impaired diastolic expansion of the ventricle ("restrictive epicarditis").²⁰ The hydrocoelom is evidence of heart failure, although the good nutritional state of the animal suggests that the disease did not negatively affect the animal for a prolonged time. Aneurysmal vascular disease is a common problem in bearded dragons; further investigation of the role of *E. pogonae* in vascular damage is indicated.¹⁶ The source of the microsporidian and the route of infection in both animals are uncertain. Bearded dragons are omnivores, and vegetables and insects usually comprise the majority of their captive diet. Insects harbor many

known microsporidian organisms.¹⁹ The possibility of transmission of microsporidians from their insect prey to bearded dragons seems plausible but alternatively, fecal contamination of fruits and vegetables has been found to be a source of microsporidia.² Vertical transmission of *Encephalitozoon* species has been documented in rabbits infected with *E. cuniculi*.⁵

Contributing Institution:

University of Minnesota Department of Veterinary Population Medicine/Minnesota Veterinary Diagnostic Laboratory - <https://www.vetmed.umn.edu/departments/veterinary-population-medicine>
<https://www.vdl.umn.edu/>

JPC diagnosis:

Heart, epicardium: Epicarditis, granulomatous and granulocytic, diffuse, chronic, severe, with marked epicardial fibrosis, and numerous intrahistiocytic and extracellular microsporidian spores, bearded dragon, lizard.

JPC comment:

The contributor provides a short review of microsporidia and *Encephalitozoon pogonae* and is the author of the most recent journal article describing this species in the bearded dragon. This case provides context for a review of microsporidian anatomy and lifecycle.

Microsporidia are a diverse group of obligate intracellular, atypical fungi. The first microsporidian was described in the nineteenth century when "pepper disease" was afflicting silkworms in Europe. That particular agent was named *Nosema bombycis* in 1857, and at the time was considered a member of the schizomycete fungi. It was moved into the new classification 'Microsporidia' in 1882, which is now composed of more than 150 described genera and more than 1200 species.⁸

The microsporidian spore, as described by the contributor, has an exospore wall, an endospore wall, sporoplasm within the spore membrane, a single or two closely associated nuclei (diplokaryon), a polarplast, the polar filament (or polar tube), and the posterior vacuole. The polar tube is often the most distinctive feature on TEM,

attached to the anchoring disk, and extends straight for a portion of the spore, then coils around the periphery of the spore. The number of coils, their arrangement, and angle of the coils are well conserved within species and are a useful diagnostic tool for identification.^{4,8}

Oncotic pressure within the spore builds to critical levels, which is likely the initiator for germination. A complex sequence of events results in the polar filament being everted from the spore, varying in length from 50-500 µm, at speeds exceeding 100 µm/s. It is currently believed that the process of germination may result in an adjacent host cell being pierced by the polar filament, and then receiving sporoplasm (the infectious material of the spore) through the polar filament. The sporoplasm develops into meronts (merogony), followed by sporogony. Meronts give rise to sporoblasts, which develop into mature spores. Many species will be found within parasitophorous vacuoles in host cells.⁸

One way to stratify the microsporidian species is based upon their ability to induce xenoma formation. Xenomas are composed of a hypertrophied host cell within which reside microsporidians at one life stage (spores, meronts, etc), and has the appearance of a cyst-like structure in the host tissue. Some species known to induce xenoma formation include *Glugea* spp, *Tetramicra* spp, *Loma* spp, and others. Others such as *Pleistophora* spp, *Nucleospora* spp, *Heterosporis* spp, and others do not induce xenoma formation.¹³

Microsporidian infections are rarely described in canines (*Encephalitozoon* spp), lagomorphs (*Encephalitozoon cuniculi* and other species), falcons (*Enterocytozoon bieneusi*), psitticines, passerines, and crocodilians (*Encephalitozoon hellem*), amphibians (*Pleistophora* spp, *Allogluzea bufonis*, others), fish (*Pleistophora* spp, *Glugea* spp), and invertebrates (various species).¹⁷ Most species noted to affect humans are zoonotic and/or waterborne, and is a particular problem in immunocompromised individuals, such as HIV/AIDS patients. In many of these cases, *Enterocytozoon bieneusi* causes lethal infections, often starting with diarrhea. However, numerous other Microsporidian

species have also been documented in humans as well.⁴

With additional research and documentation of cases, source and transmission route of *Encephalitozoon pogonae* may be ascertained, as well as whether vertical transmission is possible.

References:

1. Cali A, Neafie RC, Takvorian PM. Microsporidiosis. In: Meyers WM, et al., eds. Topics on the Pathology of Protozoan and Invasive Arthropod Diseases. Washington, DC: Armed Forces Institute of Pathology, 2011:200–223.
2. Clavo M, Carazo M, Arias ML, et al. Prevalencia de *Cyclospora* sp., *Cryptosporidium* sp., microsporidiosis y determinacion de coliformes fecales en frutas y vegetales frescos de consumo crudo en Costa Rica [Prevalence of *Cyclospora* sp., *Cryptosporidium* sp., microsporidia and fecal coliform determination in fresh fruit and vegetables consumed in Costa Rica]. *Arch Latinoam Nutr* 2004;**54**:428–432. Spanish
3. Garcia LS. Laboratory identification of the microsporidia. *J Clin Microbiol* 2002;**40**:1892–1901.
4. Han B, Weiss LM. Microsporidia: Obligate Intracellular Pathogens within the Fungal Kingdom. *Microbiol Spectr*. 2017;**5**(2): 10.1128/microbiolspec.FUNK-0018-2016. doi:10.1128/microbiolspec.FUNK-0018-2016.
5. Hunt RD, King NW, Foster HL. Encephalitozoonosis: evidence for vertical transmission. *J Infect Dis* 1972;**126**:212–214.
6. Jacobson ER, Green DE, Undeen AH, et al. Microsporidiosis in inland bearded dragons (*Pogona vitticeps*). *J Zoo Wildl Med* 1998;**29**:315–323.
7. Juan-Salles C, Garner MM, Dider ES, Serrato S, Acevedo LD, Ramos-Vera A, et al. Disseminated encephalitozoonosis in captive juvenile, cotton-top (*Saguinus oedipus*) and neonatal emperor tamarins (*Saguinus imperator*) in North America. *Vet Pathol*. 2006;**43**:438-446.
8. Keeling PJ, Fast NM. Microsporidia: Biology and Evolution of Highly Reduced Intracellular Parasites. *Annu. Rev. Microbiol*. 2002;**56**:93-116.
9. Lom J, Nilsen F. Fish microsporidian: fine structural diversity and phylogeny. *Int J Parasitol* 2003;**33**:107–127.

10. Martel-Arquette A, Chen S, Hempstead J, et al. Microsporidial keratoconjunctivitis in a pet bearded dragon (*Pogona vitticeps*). *J Exotic Pet Med* 2017;**26**:257–262.
11. Phelps NBD, Mor SK, Armien AG, et al. Description of the microsporidian parasite, *Heterosporis sutherlandae* n. sp., infecting fish in the Great Lakes region. *PLoS One* 2015;**10**:e0132027.
12. Richter B, Csokai J, Graner I, et al. Encephalitozoonosis in two inland bearded dragons (*Pogona vitticeps*). *J Comp Pathol* 2013;**148**:278–282.
13. Rodriguez-Tovar LE, Speare DJ, Markham F. Fish microsporidia: Immune response, immunomodulation and vaccination. *Fish and Shellfish Immunology*. 2011;**30**:999–1006.
14. Shibasaki K, Tokiwa T, Sukegawa A, et al. First report of fatal disseminated microsporidiosis in two inland bearded dragons *Pogona vitticeps* in Japan. *JMM Case Rep* 2017;**4**:e005089.
15. Sokolova YY, Sakaguchi K, Paulsen DB. Establishing a new species *Encephalitozoon pogonae* for the microsporidian parasite of bearded dragon *Pogona vitticeps* Ahl 1927 (Reptilia, Squamata, Agamidae). *J Eukary Microbiol* 2016;**63**:524–535.
16. Sweet CR, Linnetz E, Golden E. What is your diagnosis? Pericardial effusion, cardiac mass, or cardiomegaly secondary to heart diseases. *J Am Vet Med Assoc* 2009;**234**:1259–1260.
17. Terio KA, McAloose D, St. Leger, J. *Pathology of Wildlife and Zoo Animals*. San Diego, CA: Elsevier. 2018.
18. Vávra J, Lukeš J. Microsporidia and ‘the art of living together’. *Adv Parasitol* 2013;**82**:253–319.
19. Vergeneau-Grosset C, Larrat S. Microsporidiosis in vertebrate companion exotic animals. *J Fungi* (Basel) 2015;**2**:E3.
20. Wünschmann A, Armien AG, Childress AL, et al. Intrapericardial *Encephalitozoon pogonae*-associated arteritis with fatal hemopericardium in two juvenile bearded dragons. *J Vet Diagn Invest* 2019;**31**:467–470.